

Structural stability and structural imitation of $\text{La}_2\text{Co}_{17-x}\text{M}_x$ (M = Mn, Mo, Nb, Ti, V, Al, Cr, Ni and Si)

H. Chang^{1,a}, N.X. Chen^{2,3}, J.K. Liang^{1,4}, and G.H. Rao¹

¹ Institute of Physics and Center for Condensed Matter Physics, Chinese Academy of Sciences, Beijing 100080, PR China

² Department of Physics, Tsinghua University, Beijing, 100084, PR China

³ Institute of Applied Physics, Beijing University of Science and Technology, Beijing, 100083, PR China

⁴ International Center for Materials Physics, Chinese Academy of Sciences, Shenyang 110016, PR China

Received 1st November 2002 / Received in final form 17 February 2003

Published online 23 May 2003 – © EDP Sciences, Società Italiana di Fisica, Springer-Verlag 2003

Abstract. The structural stability of $\text{La}_2\text{Co}_{17-x}\text{M}_x$ (M = Mn, Mo, Nb, Ti, V, Al, Cr, Ni and Si) based on the interatomic potential has been studied. The calculated site preference of the third element M is found to be the 6c site, which is in agreement with the experiments. In the calculations, if the crystal cohesive energy of $\text{La}_2\text{Co}_{16}\text{Mn}$ is taken as the highest one in the crystallization of $\text{La}_2\text{Co}_{17-x}\text{M}_x$, the lowest content x of the third element M (M = Mn, Mo, Nb, Ti and V) required to stabilize $\text{La}_2\text{Co}_{17-x}\text{M}_x$, is near that found in the experiments. The differences of the cell parameters between the calculated and the experimental values are less than 0.4%. The differences of the atomic parameters for Co (or M) between the calculated and the experimental values are about or even smaller than 1%, and that of La is about 3%. Because the energies of $\text{La}(\text{Co}_{1-x}\text{Al}_x)_{13}$ are lower than those of $\text{La}_2(\text{Co}_{1-x}\text{Al}_x)_{17}$, $\text{La}_2(\text{Co}_{1-x}\text{Al}_x)_{17}$ could not be formed in the experiments. In the calculations, with either a range of deformation of the structure or the reconstruction of the initial structure $\text{La}_2\text{Co}_{17}$ from LaCo_5 , the same results including the cohesive energy curves and the crystallographic parameters can be retrieved after the action of the interatomic potentials.

PACS. 64.30.+t Equations of state of specific substances – 75.50.Cc Other ferromagnetic metals and alloys – 64.60.-i General studies of phase transitions – 64.70.-p Specific phase transitions

Introduction

R_2Co_{17} forms a very important series of permanent magnetic materials with a high saturation magnetization and a high Curie temperature. Except for La, all the other rare earths can form the binary compounds R_2Co_{17} . Liu *et al.* has successfully synthesized the single phased $\text{La}_2\text{Co}_{17-x}\text{M}_x$ (M = Mn, Mo, Nb, Ti and V) [1–3]. They not only have a high Curie temperature, but also have easy axial anisotropy [1–3]. That makes them candidates for permanent magnetic applications. The investigation of the phase formation of $\text{La}_2\text{Co}_{17-x}\text{M}_x$ by theoretical calculation should provide guidance for the synthesis of the new $\text{La}_2\text{Co}_{17-x}\text{M}_x$ compounds. In the past, the atomic radius and the enthalpy of formation were widely used to predict the phase formation [4]. However, these methods can only give a semi-experimental estimation of the phase formation and often these methods are inaccurate. Moreover, they have shortcomings in that they do not take the elastic deformation and the crystal structure dependent contribution into account. In the study of the metals and the in-

termetallics, the interatomic potentials combined with the different crystal structures have been successfully used. It is the local atomic environment that determines if the energy of a compound is low enough to form a compound with a certain structure. Taking an energy viewpoint is an effective shortcut to investigate the structural stability and the site preference. However, since it is very difficult to obtain the potentials in the rare earth-containing compounds, little work has been done on them. Chen *et al.* proposed the lattice inversion method to obtain the interatomic pair potential, which is very timesaving and effective [5]. In this paper, we calculated the stabilizing effects of the third elements M (M = Mn, Mo, Nb, Ti, V, Al, Cr, Ni and Si) on $\text{La}_2\text{Co}_{17-x}\text{M}_x$ based on Chen's Lattice inversion method.

Calculation method

In 1980, Carlsson *et al.* proposed a method to obtain the cohesive energy of the metal by an *ab initio* calculation [6]. The interatomic pair potentials could be inferred from the

^a e-mail: hchang@aphy.iphy.ac.cn

calculated cohesive energy curves by inversion. The calculation of pair potentials is free of any variable parameter. The work is based on the assumptions that (a) the cohesive energy is a sum of the pair interaction energies, and (b) the cohesive energy derived from the electronic structure calculations is a function of the volume. But it has some vital shortcomings, for examples, it includes infinite summations with each summation having infinite terms. Based on the same assumption, Chen proposed the calculation of the pair potential in another way [5]. The special characteristics are (a) the calculation of the cohesive energy is based on the virtual structure and is deduced from the total energy of the sublattice, (b) the inversion method is a rigorous and concise way to obtain the interatomic potentials, (c) the interatomic potential between the different atoms can also be obtained by the same procedure, and (d) it is convenient for the analysis since the inversion coefficient of the different materials with the identical structure is uniform.

A brief introduction of the lattice inversion theorem is proposed as follows [5]. Suppose that the crystal cohesive energy obtained by the first principle calculation is expressed as

$$E(\chi) = \frac{1}{2} \sum_{n=1}^{\infty} r_0(n) \Phi(b_0(n)\chi), \quad (1)$$

where χ is the near-neighbor distance, $r_0(n)$ is the n th neighbor coordination number, $b_0(n)\chi$ is the distance between the central reference atom and its n th neighbor, and $\Phi(b_0(n)\chi)$ is the pair potential. A multiplicative closed semigroup $b(n)$ is formed by the self-multiplicative process from $b_0(n)$. In this process, a lot of virtual lattice points are involved, but the corresponding virtual coordination number is zero. In the $b(n)$, for any two integers m and n , there is a sole integer k such that $b(k) = b(m)b(n)$. Hence, equation (1) can be rewritten as

$$E(\chi) = \frac{1}{2} \sum_{n=1}^{\infty} r(n) \Phi(b(n)\chi) \quad (2)$$

where

$$r(n) = \begin{cases} r_0(n) (b_0^{-1}[b(n)]) & \text{if } b(n) \in \{b_0(n)\} \\ 0 & \text{if } b(n) \notin \{b_0(n)\}. \end{cases} \quad (3)$$

Then the general equation for the interatomic pair potential obtained from the inversion can be expressed as

$$\Phi(\chi) = 2 \sum_{n=1}^{\infty} I(n) E(b(n)\chi) \quad (4)$$

where $I(n)$ has the characteristics of

$$\sum_{b(d)b(n)} I(d) r \left(b^{-1} \left[\frac{b(n)}{b(d)} \right] \right) = \delta_{nl}. \quad (5)$$

$I(n)$ is uniquely determined by a geometrical crystal structure, not related to the concrete element category. Thus,

the interatomic pair potentials can be obtained from the known cohesive energy function $E(\chi)$.

In order to obtain the necessary interatomic potentials, some simple and virtual structures are designed to calculate the cohesive energy curve $E(\chi)$. The cohesive energy is calculated based on the norm-conserving pseudopotential method. The generalized gradient approximation is used in the exchange-correlation term of the density functional theory. For the electronic structure of the rare earth element, the valence electrons are f -electrons are in valence. More than 80 k -points in an irreducible Brillouin zone are taken into account in a self-consistent calculation and the energy convergence error is 0.200×10^{-5} eV/atom.

First, by assuming the virtual structure of Co to be the CsCl structure with two simple cubic sublattices Co₁ and Co₂, the cohesive energy is expressed as

$$\begin{aligned} E(\chi) &= E_{\text{Co}}^{\text{BCC}}(\chi) - E_{\text{Co}_1}^{\text{SC}}(\chi) - E_{\text{Co}_2}^{\text{SC}}(\chi) \\ &= \sum_{i,j,k \neq 0}^{\infty} \Phi_{\text{Co-Co}} \\ &\quad \times \sqrt{\left[\frac{4}{3} \left[\left(i - \frac{1}{2} \right)^2 + \left(j - \frac{1}{2} \right)^2 + \left(k - \frac{1}{2} \right)^2 \right] \chi \right]} \end{aligned} \quad (6)$$

where χ is the near-neighbor distance in the BCC structure, $E_{\text{Co}}^{\text{BCC}}(\chi)$ represents the total energy curve with the BCC structure, $E_{\text{Co}_1}^{\text{SC}}(\chi)$ or $E_{\text{Co}_2}^{\text{SC}}(\chi)$ is the total energy function with a simple cubic structure. Then, $E(\chi)$ is the cohesive energy function of one Co₁ atom with all the other Co₂ atoms. Here, the Co₂ atoms form a simple cubic structure, and one Co₁ atom is located at the center of the cube. Then, the interatomic potential $\Phi_{\text{Co-Co}}$ can be obtained with the lattice inversion technique described above.

However, it is hard to obtain the total energy curve of La-Co with the *ab initio* calculation. The lattice constant, module constant and total energy of La₃Co with L1₂ structure are calculated near the equilibrium. By subtracting the contribution of La-La and Co-Co in the structure, the partial cohesive energy of La-Co can be obtained. Then, $\Phi_{\text{La-Co}}$ can be deduced from the lattice inversion. Similarly, the potentials related to the other element M (M = Mn, Mo, Nb, Ti, V, Al, Cr, Ni and Si) can be derived by the same methods. The potentials can be fitted with the Morse function

$$\Phi(\chi) = D_0(u^2 - 2u), \quad u = e^{-\alpha(\chi - R_0)}, \quad \gamma = 2R_0\alpha$$

where D_0 , R_0 , γ are potential parameters. All the potential curves are shown in Figure 1 for $\Phi_{\text{La-M}}$ (M = Mn, Mo, Nb, Ti, V, Al, Si, Ni and Cr), and Figure 2 for $\Phi_{\text{Co-M}}$ (M = Mn, Mo, Nb, Ti, V, Al, Si, Ni and Cr). Based on these interatomic potentials, the cohesive energy for the actual complex structures can be obtained.

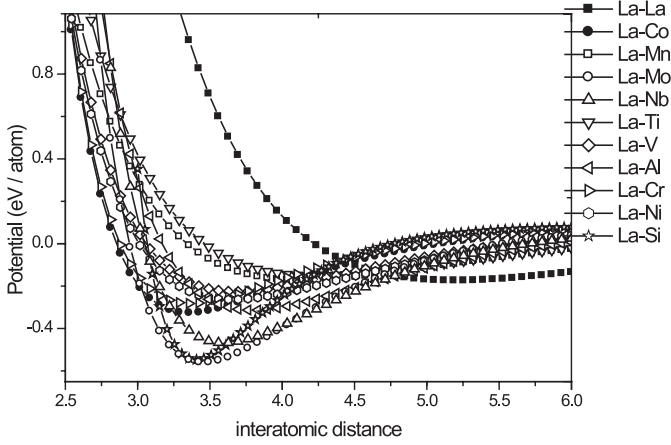


Fig. 1. The potential curves of $\Phi_{\text{La-M}}$ ($M = \text{Co}, \text{Mn}, \text{Mo}, \text{Nb}, \text{Ti}, \text{V}, \text{Al}, \text{Cr}, \text{Ni}$ and Si).

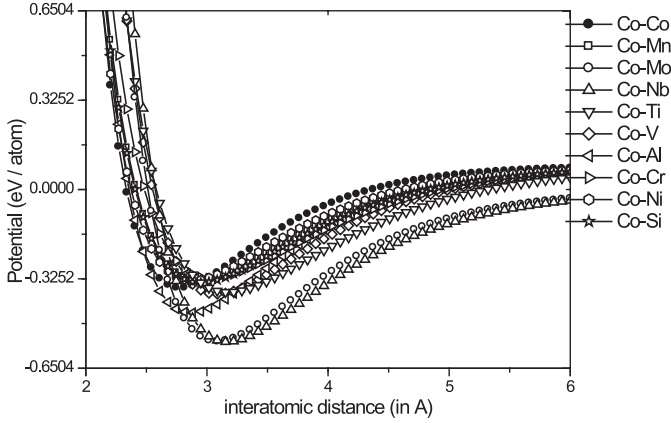


Fig. 2. The potential curves of $\Phi_{\text{Co-M}}$ ($M = \text{Co}, \text{Mn}, \text{Mo}, \text{Nb}, \text{Ti}, \text{V}, \text{Al}, \text{Cr}, \text{Ni}$ and Si).

Results and discussion

Structural stability of $\text{La}_2\text{Co}_{17-x}\text{M}_x$ ($M = \text{Mn}, \text{Mo}, \text{Nb}, \text{Ti}, \text{V}, \text{Al}, \text{Si}, \text{Ni}$ and Cr)

In the experiments, $\text{La}_2\text{Co}_{17-x}\text{M}_x$ ($M = \text{Mn}, \text{Mo}, \text{Nb}, \text{Ti}$ and V) could be stabilized in the rhombohedral $\text{Th}_2\text{Zn}_{17}$ -type structure, whereas $\text{Th}_2\text{Zn}_{17}$ -type $\text{La}_2\text{Co}_{17-x}\text{M}_x$ could not be stabilized with $M = \text{Cr}, \text{Ni}, \text{Si}, \text{Al}$ [1–3]. The transition metal may occupy four kinds of site, 6c, 9d, 18h and 18f, and M substitutes for the dumbbell pair of Co atoms at the 6c site. In the calculation, if the substitution of M for Co makes the cohesive energy of $\text{La}_2\text{Co}_{17-x}\text{M}_x$ low enough, the third element M could stabilize the compound. Furthermore, M would preferentially occupy the site, so that the cohesive energy would decrease most strongly. Figure 3 shows the cohesive energy of $\text{La}_2\text{Co}_{17-x}\text{Ti}_x$ with Ti at the 6c, 9d, 18h and 18f sites, respectively. In the calculations, the substitution of Ti for Co at all the four sites 6c, 9d, 18h and 18f decreases the cohesive energy of $\text{La}_2\text{Co}_{17-x}\text{Ti}_x$. When Ti enters into the 6c site, the cohesive energy of $\text{La}_2\text{Co}_{17-x}\text{Ti}_x$ is the lowest. Then, the 6c site should be preferentially occupied by Ti, which agrees with the experiments [1]. When

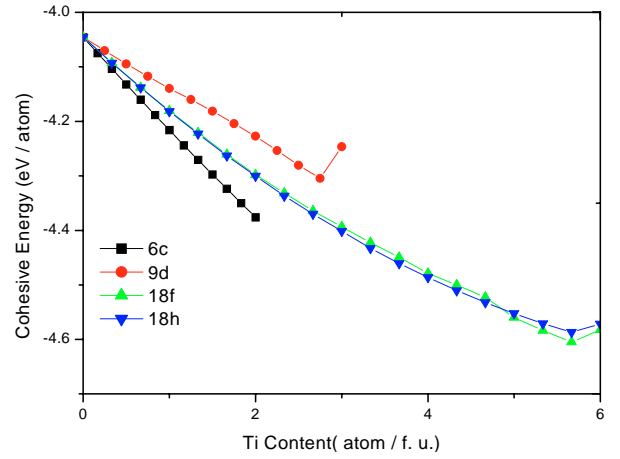


Fig. 3. The cohesive energy of $\text{La}_2\text{Co}_{17-x}\text{Ti}_x$ with Ti at the 6c, 9d, 18h and 18f sites, respectively.

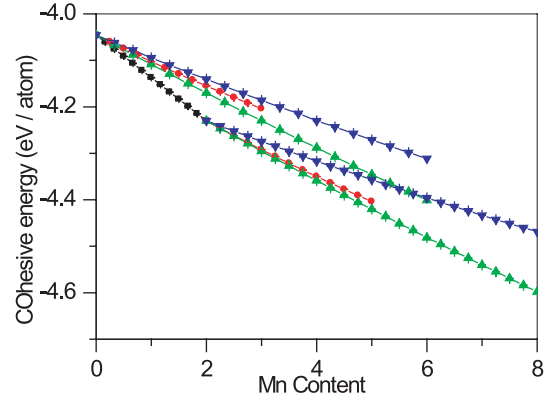


Fig. 4. The cohesive energy of $\text{La}_2\text{Co}_{17-x}\text{Mn}_x$ with Mn at the 6c, 9d, 18h and 18f sites for $x \leq 2$, and for $x > 2$ the cohesive energy of $\text{La}_2\text{Co}_{17-x}\text{Mn}_x$ with the 6c site fully occupied by Mn and the rest of Mn at the 9d, 18h and 18f sites, respectively.

any of the other third elements M ($M = \text{Mn}, \text{Mo}, \text{Nb}, \text{V}, \text{Al}, \text{Cr}, \text{Ni}$ and Si) is substituted for Co, the cohesive energy of $\text{La}_2\text{Co}_{17-x}\text{M}_x$ is also the lowest with M at the 6c site. That indicates the third elements M ($M = \text{Mn}, \text{Mo}, \text{Nb}, \text{V}, \text{Al}, \text{Cr}, \text{Ni}$ and Si) prefer to occupy the 6c site, which is just as in the experiments for $M = \text{Mn}, \text{Mo}, \text{Nb}, \text{V}$ [2,3]. The 6c site, fully occupied by M corresponds to $x = 2$ in $\text{La}_2\text{Co}_{17-x}\text{M}_x$. Unlike the other M, $\text{La}_2\text{Co}_{17-x}\text{Mn}_x$ can crystallize with x up to 4. Figure 4 shows the cohesive energy of $\text{La}_2\text{Co}_{17-x}\text{Mn}_x$. For $x > 2$, based on the assumption that the 6c site is fully occupied by Mn, the energy of $\text{La}_2\text{Co}_{17-x}\text{Mn}_x$ decreases with the increasing Mn content, and it has the lowest value with Mn substituting for Co at the 18f site. In the experiments, no report about the site preference of Mn with $x > 2$ is found. The substitution of M ($M = \text{Mn}, \text{Mo}, \text{Nb}, \text{Ti}, \text{V}, \text{Al}, \text{Cr}, \text{Ni}$ and Si) for Co at the 6c site could decrease the energy of $\text{La}_2\text{Co}_{17-x}\text{M}_x$ more or less, as shown in Figure 5. Taking the energy of $\text{La}_2\text{Co}_{16}\text{Mn}$ as the boundary, the energy curves with Cr, Ni and Si substituting for Co at the 6c site lie above those with Mn, Mo, Nb, Ti, V and Al substituting for Co. Considering that Al, Cr,

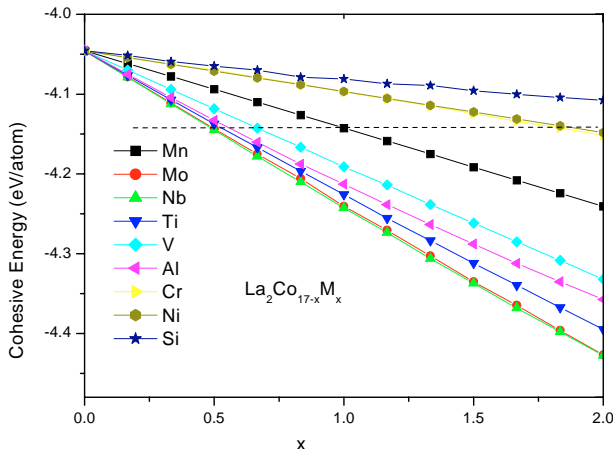


Fig. 5. The cohesive energy of $\text{La}_2\text{Co}_{17-x}\text{M}_x$ ($M = \text{Mn}, \text{Mo}, \text{Nb}, \text{Ti}, \text{V}, \text{Al}, \text{Cr}, \text{Ni}$ and Si) with M substituting for Co at the 6c site, the dashed line denotes the contour line of the energy of $\text{La}_2\text{Co}_{16}\text{Mn}$.

Ni and Si can not stabilize $\text{La}_2\text{Co}_{17-x}\text{M}_x$, $\text{La}_2\text{Co}_{17-x}\text{Al}_x$ is an exception. In the experiments, both LaCo_{13} and $\text{LaCo}_{13-x}\text{Al}_x$ can be synthesized, but $\text{La}_2\text{Co}_{17}$ cannot be formed [1–3,7]. Figure 6 shows the cohesive energy of $\text{La}(\text{Co}_{1-x}\text{Al}_x)_{13}$ with Al substituting for Co at the 96i site and that of $\text{La}_2(\text{Co}_{1-x}\text{Al}_x)_{17}$ with Al at the 6c site. In both the experiment and the calculation of $\text{La}(\text{Co}_{1-x}\text{Al}_x)_{13}$, Al occupies the 96i site [7,8], and in the calculation of $\text{La}_2(\text{Co}_{1-x}\text{Al}_x)_{17}$, the cohesive energy is the lowest with Al at the 6c site. Although the substitution of Al for Co decreases the energy of $\text{La}_2(\text{Co}_{1-x}\text{Al}_x)_{17}$, the energy of $\text{La}(\text{Co}_{1-x}\text{Al}_x)_{13}$ is even lower than that of $\text{La}_2(\text{Co}_{1-x}\text{Al}_x)_{17}$. That indicates $\text{La}(\text{Co}_{1-x}\text{Al}_x)_{13}$ is more stable than $\text{La}_2(\text{Co}_{1-x}\text{Al}_x)_{17}$.

The lowest content x of the third element M required to stabilize the compounds $\text{La}_2\text{Co}_{17-x}\text{M}_x$ ($M = \text{Mn}, \text{Mo}, \text{Nb}, \text{Ti},$ and V) can also be estimated from the calculations. In the experiments, the lowest Mn content, which can stabilize $\text{La}_2\text{Co}_{17-x}\text{M}_x$, is $x = 1.0$. The energy of $\text{La}_2\text{Co}_{16}\text{Mn}$ can be taken as the highest in $\text{La}_2\text{Co}_{17-x}\text{M}_x$, and $\text{La}_2\text{Co}_{17-x}\text{M}_x$ ($M = \text{Mn}, \text{Mo}, \text{Nb}, \text{Ti}, \text{V}, \text{Al}, \text{Cr}, \text{Ni}$ and Si) can be synthesized in the experiments with the energy lower than $\text{La}_2\text{Co}_{16}\text{Mn}$. Based on this, it is deduced that $\text{La}_2\text{Co}_{17-x}\text{V}_x$ can form with $x > 0.7$, and $\text{La}_2\text{Co}_{17-x}\text{M}_x$ ($M = \text{Mo}, \text{Nb}$ and Ti) can form with $x > 0.5$. In the experiments, $\text{La}_2\text{Co}_{17-x}\text{V}_x$ crystallizes in a single phased $\text{Th}_2\text{Zn}_{17}$ -type structure with $0.8 < x < 1.2$, and $\text{La}_2\text{Co}_{17-x}\text{Mo}_x$ with $0.4 < x < 1.2$, and $\text{La}_2\text{Co}_{17-x}\text{Nb}_x$ with $0.3 < x < 0.6$, and $\text{La}_2\text{Co}_{17-x}\text{Ti}_x$ with $0.8 < x < 1.2$. Although the calculated limits of the M content are not exactly the same as those in the experiments, the calculated results reflect the trend that the amount of M , which are needed to stabilize $\text{La}_2\text{Co}_{17-x}\text{M}_x$, increases in the order $\text{Nb}, \text{Mo}, \text{Ti}, \text{V}$ and Mn . Furthermore, when $M = \text{Cr}$ and Ni , the proportion of the third element must be as high as $x > 1.9$ to make the energy of $\text{La}_2\text{Co}_{17-x}\text{M}_x$ ($M = \text{Cr}$ and Ni) as low as that of $\text{La}_2\text{Co}_{16}\text{Mn}$, and for $M = \text{Si}$, the amount of x should

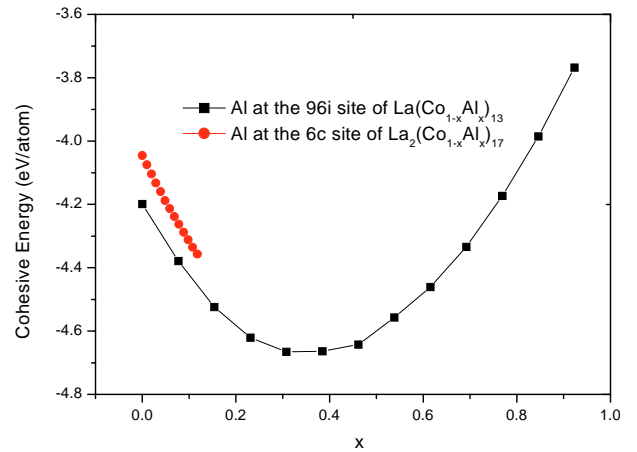


Fig. 6. The cohesive energy of $\text{La}_2\text{Co}_{17-x}\text{Al}_x$ with Al substituting for Co at the 6c site and $\text{LaCo}_{13-x}\text{Al}_x$ with Al substituting for Co at the 96i site, respectively.

be $x > 2$. In the experiments, $\text{La}_2\text{Co}_{17-x}\text{M}_x$ ($M = \text{Cr}, \text{Ni}$ and Si) have been studied only with $x = 0.5, 1.0,$ and 1.5 , and the effort to form this type of compounds resulted in failure [3].

Crystallographic properties and magnetic properties

In the calculation, not only the structural stability and the site preference of the third element can be judged by the energy of the system, but the crystallographic parameters can also be obtained. Figure 7 shows the cell parameters of $\text{La}_2\text{Co}_{17-x}\text{M}_x$ ($M = \text{Mo}, \text{Mn}, \text{Nb}, \text{Ti}, \text{V}$) obtained from both the experiments and the calculations. The differences of both a and c between the experiments and the calculations are less than 0.4%, which is acceptable. In the experiments and the calculations, the cell parameters a and c of $\text{La}_2\text{Co}_{17-x}\text{M}_x$ ($M = \text{Mn}, \text{Mo}, \text{Nb}, \text{Ti}$ and V) increase with the increasing content of M . That is consistent with the case that the atomic sizes of all the third elements $M = \text{Mn}, \text{Mo}, \text{Nb}, \text{Ti}$ and V are larger than that of Co . In the calculations, with the same proportion of the third elements M , the parameters a and c increase in the order of $\text{Nb} > \text{Ti} (\approx \text{Mo}) > \text{V} > \text{Mn}$, which is also the order of the atomic size. But in the experiments, the cell parameter a of $\text{La}_2\text{Co}_{17-x}\text{Mn}_x$ is larger than those of $\text{La}_2\text{Co}_{17-x}\text{V}_x, \text{La}_2\text{Co}_{17-x}\text{Mo}_x$ and $\text{La}_2\text{Co}_{17-x}\text{Ti}_x$. This may be due to the magnetostriction, which is widely observed in magnetic materials. Unlike the other third elements M ($M = \text{Mo}, \text{Nb}, \text{Ti}$ and V), Mn has an intrinsic magnetic moment. In the calculations, the magnetic interaction is not taken into account.

Table 1 lists the calculated atomic positions in a unit cell of $\text{La}_2\text{Co}_{16}\text{Ti}$ and $\text{La}_2\text{Co}_{16}\text{V}$ with the experimental data in brackets. The differences between the experimental and the calculated atomic positions at all the Co (M) sites are about or even smaller than 1%, and the difference at the La (6c) site is about 3%.

In order to verify if the final states are stable, all the atoms in both $\text{La}_2\text{Co}_{16}\text{Ti}$ and $\text{La}_2\text{Co}_{16}\text{V}$ are moved randomly in the range of less than 0.3 Å, the same cell

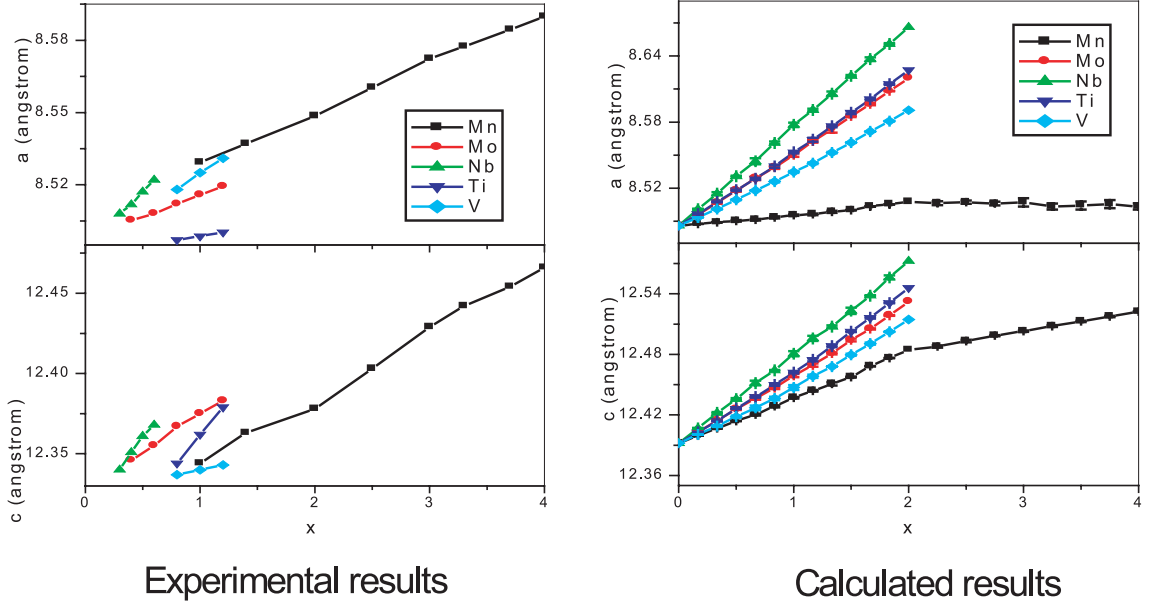


Fig. 7. The cell parameters a and c of $\text{La}_2\text{Co}_{17-x}\text{M}_x$ ($M = \text{Mn}, \text{Mo}, \text{Nb}, \text{Ti}$ and V) obtained from both the calculations and the experiments.

Table 1. The calculated atomic positions in a unit cell of $\text{La}_2\text{Co}_{16}\text{Ti}$ and $\text{La}_2\text{Co}_{16}\text{V}$ with the experimental data in brackets.

	atom	site	x/a	y/b	z/c
	La	6c	0	0	0.338(0.3471)
$\text{La}_2\text{Co}_{16}\text{Ti}$	Co+Ti	6c	0	0	0.098(0.0961)
	Co	9d	0.5	0	0.5
	Co	18h	0.501(0.5000)	0.002(0.0000)	0.151(0.1548)
	Co	18f	0.291(0.2893)	0	0
$\text{La}_2\text{Co}_{16}\text{V}$	La	6c	0	0	0.337(0.3469)
	Co+V	6c	0	0	0.096(0.0925)
	Co	9d	0.5	0	0.5
	Co	18h	0.501(0.5000)	0.002(0.0000)	0.151(0.1553)
	Co	18f	0.291(0.2888)	0	0

parameters and atomic positions are retrieved after the action of the interatomic potential. The structure of R_2Co_{17} is the crystallographic derivative of that of RCO_5 . The calculations are also carried out with the initial structure $\text{La}_2\text{Co}_{17}$ constructed from LaCo_5 . By substituting one third of the La atoms in LaCo_5 by a pair of Co atoms, which is usually called the dumb-bell pair, LaCo_5 is transformed into $\text{La}_2\text{Co}_{17}$. Because the transformation is geometric, the structure of $\text{La}_2\text{Co}_{17}$ formed in this way is rather different from the experimental one. With this initial $\text{La}_2\text{Co}_{17}$, by substituting M ($M = \text{Mn}, \text{Mo}, \text{Nb}, \text{Ti}, \text{V}, \text{Al}, \text{Cr}, \text{Ni}$ and Si) for Co, all the calculated results including the cohesive energy, the cell and the atomic parameters being the same as in the above calculations. It confirms that the current calculations are reliable within a reasonable range of deformation and that the two kinds of structures are fairly closely related.

In the experiments, it is exciting to observe that the easy magnetization direction (EMD) of $\text{La}_2\text{Co}_{17-x}\text{Ti}_x$ and $\text{La}_2\text{Co}_{17-x}\text{V}_x$ is along c -axis [1–3], which is a prerequi-

site for a permanent magnetic material. Generally, the magnetocrystalline anisotropy can be divided into two parts, the rare earth sublattice contribution and the transition metal sublattice contribution. In $\text{La}_2\text{Co}_{17-x}\text{M}_x$, La has no magnetic moment, and the easy-axis anisotropy of $\text{La}_2\text{Co}_{17-x}\text{M}_x$ is entirely due to the transition metal sublattice. Since $\text{La}_2\text{Co}_{17}$ does not exist, R_2Co_{17} ($\text{R} = \text{Y}, \text{Gd}$, and Lu), whose magnetocrystalline anisotropy are also due to the transition metal sublattice, are used in the analysis. In their parent compounds RCO_5 ($\text{R} = \text{Y}, \text{Gd}$ and Lu), the EMDs are along c -axis [9–11]. However, in the compounds R_2Co_{17} ($\text{R} = \text{Y}, \text{Gd}$ and Lu), which has the 6c dumb-bell Co atoms, the EMDs lie in the basal plane. That indicates that the 6c dumb-bell Co atoms play a determinant role on the easy-plane anisotropy. Although the EMD of $\text{La}_2\text{Co}_{17}$ can not be determined, the substitution of M for Co at the dumb-bell sites of $\text{La}_2\text{Co}_{17-x}\text{M}_x$ ($M = \text{Mo}, \text{Mn}, \text{Nb}, \text{Ti}, \text{V}$) weakens the easy-plane anisotropy resulting from the dumb-bell Co atoms, thus inducing a favorable uniaxial anisotropy. In fact, that is not a unique phenomenon,

and the substitutions of Mo for Co in Y_2Co_{17} and Mn for Co in Gd_2Co_{17} also change their EMDs from the easy-plane to c -axis [12,13].

Conclusion

The calculations based on the interatomic potential can give a rather good imitation of the crystallographic stability and the crystallographic parameters. It should be useful in the prediction of new $La_2Co_{17-x}M_x$ and other compounds. If the magnetic interaction can be added in the interatomic potential, the calculations on the magnetic compounds would be better.

This work is supported by the State Key Project of Fundamental Research, No G2000067101, G1998061307, and G1998061303. One of the authors, H.C., would like to thank Professor J. Shen for constructive discussions.

References

1. Q. Liu, J. Liang, G. Rao, W. Tang, J. Sun, X. Chen, B. Shen, *Appl. Phys. Lett.* **71**, 1869 (1997)
2. Q.L. Liu, J.K. Liang, J. Xu, X.L. Chen, Y. Shi, B.G. Shen, *J. Phys. Cond. Matt.* **9**, 9947 (1997)
3. Q.L. Liu, J.K. Liang, F. Huang, Y. Chen, G.H. Rao, X.L. Chen, B.G. Shen *J. Phys. Cond. Matt.* **48**, 9797 (1999)
4. J.K. Liang, Q.L. Liu, F. Huang, G.H. Rao, X.L. Chen, *Prog. Natural Sci.* **12**, 81 (2002)
5. N.X. Chen, Z.D. Chen, Y.C. Wei, *Phys. Rev. E* **55**, R5 (1997)
6. A.E. Carlsson, C.D. Galett, H. Ehrenreich, *Philos. Mag. A* **41**, 241 (1980)
7. H. Ido, J.C. Sohn, F. Pourarian, S.F. Cheng, W.E. Wallace, *J. Appl. Phys.* **67**, 4978 (1990)
8. H. Chang, N. Chen, J. Liang, G. Rao, *J. Phys. Cond. Matt.* **15**, 109 (2003)
9. X.C. Kou, T.S. Zhao, R. Grössinger, *Phys. Rev. B* **46**, 6225 (1992)
10. R.S. Perkins, P. Fischer, *Solid State Commun.* **20**, 1013 (1976)
11. H.J. Schaller, R.S. Craig, W.E. Wallace, *J. Appl. Phys.* **43**, 3161 (1972)
12. L. Zhang, Y.N. Liang, D.C. Zeng, J.C.P. Klaasse, E. Brück, Z.Y. Liu, F.R. Boer, K.H.J. Buschow, *Physica B* **291**, 110 (2000)
13. Z.G. Sun, S.Y. Zhang, H.W. Zhang, B.G. Shen, *J. Alloys Comp.* **322**, 69 (2001)